Available online at www.sciencedirect.com
ScienceDirect
Bioorganic & Medicinal Chemistry Letters 18 (2008) 318–323
Bioorganic & Medicinal Chemistry Letters

Biphenyl amide p38 kinase inhibitors 1: Discovery and binding mode

Richard M. Angell,[†] Paul Bamborough,[*] Anne Cleasby,[‡] Stuart G. Cockerill,[†] Katherine L. Jones, Christopher J. Mooney, Donald O. Somers and Ann L. Walker

GlaxoSmithKline R&D, Medicines Research Centre, Gunnels Wood Road, Stevenage, Hertfordshire SG1 2NY, UK

Received 8 August 2007; revised 16 October 2007; accepted 22 October 2007
Available online 19 November 2007

Abstract—The biphenyl amides (BPAs) are a novel series of p38 MAP kinase inhibitors. The discovery of the series through structure-based focused screening is described, and the binding mode of the compounds is explained with reference to X-ray crystal structures.

The p38α mitogen-activated protein kinase was first identified in human monocytes as the target for a class of cytokine suppressive anti-inflammatory compounds.[1] From its central position in the cell signalling pathway, p38α regulates the expression of many pro-inflammatory cytokines including IL-1, IL-6 and TNFα. These are implicated in disease-associated processes of inflammation and progressive cartilage and bone destruction in rheumatoid arthritis. p38α inhibitors suppress the production of cytokines in vitro and have anti-inflammatory activity in vivo in models of rheumatoid arthritis and other diseases.[2] It is unclear whether the failure of some p38α inhibitors in clinical trials was due to target-related toxicity or off-target effects related to the selectivity profiles of the clinical candidates. More selective and structurally distinct inhibitors may avoid some of the problems of previous series. Much effort continues to be devoted to the discovery of potent, selective p38α inhibitors for the clinical management of rheumatoid arthritis.[3]

Quinolines and quinazolines are well documented as tyrosine kinase inhibitors (e.g., SKI-606, a Src/Abl inhibitor, or the VEGFR inhibitor ZD4190.[4,5]). The 4-anilino quinoline series, examplified by compound **1**, emerged as potent inhibitors of Lck tyrosine kinase (see Table 1 for enzyme inhibition data).[6,7] As part of the investigation into 4-anilino quinolines, the X-ray structure of **1** was determined in complex with p38α, a protein kinase used as a crystallographic surrogate for Lck.[8] The conformation of p38α in complex with **1** is broadly the same as that in the complex with SB-203580 and in the apo structure, with no major rearrangements in the protein structure.[9,10]

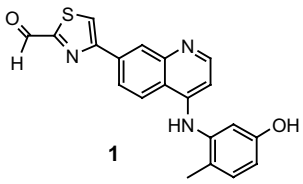

1

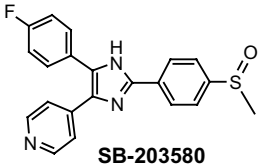

SB-203580

The binding mode of **1** is illustrated in Figure 1. Overall, it is similar to the published structure of a 4-anilino quinazoline bound to p38α.[11] The conformation of the ligand is extended, with the aniline ring projecting into the back-pocket of the ATP-binding site adjacent to the 'gatekeeper' residue Thr106. Compound **1** makes

Keywords: p38 kinase; p38 alpha; p38; CSBP; MAP kinase; Inhibitors; Biphenyl amide; BPA; Biphenyl amides; BPAs; Protein kinase X-ray structure; Binding mode; Pharmacophore search; Focused screen; Virtual screening; Structure-based drug design; kinase selectivity.
* Corresponding author. Tel.: +44 0 1438 763246; fax: +44 0 1438 763352; e-mail: paul.a.bamborough@gsk.com
† Current address: Arrow Therapeutics, Britannia House, 7 Trinity Street, London SE1 1DA, UK.
‡ Current address: Astex Therapeutics, 436 Cambridge Science Park, Milton Road, Cambridge CB4 0QA, UK.

0960-894X/$ - see front matter © 2007 Elsevier Ltd. All rights reserved.
doi:10.1016/j.bmcl.2007.10.076

Table 1. Activities of compounds **1**–**4** against p38α, JNK3 and Lck[13] (μM)

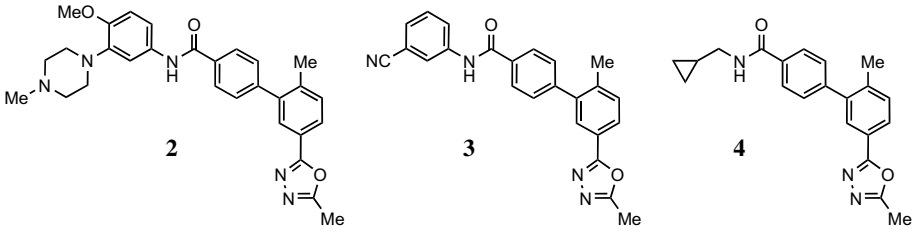

Compound	p38α		Lck		JNK3	
	IC_{50}	K_i	IC_{50}	K_i	IC_{50}	K_i
1	2.5	0.40	0.059	0.020	>16	>4
2	10	1.6	8.4	2.8	>16	>4
3	1.5	0.24	>16	>5.4	>16	>4
4	3.0	0.48	>16	>5.4	>16	>4

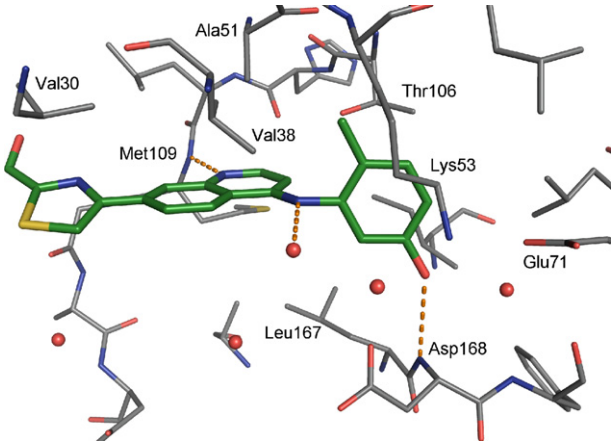

Figure 1. The binding mode of compound **1** in p38α. Hydrogen bonds are indicated by orange dotted lines.

two direct hydrogen-bonds to the protein. The first is between the quinoline nitrogen and the amide backbone NH atom of Met109 (with a distance of 2.8 Å between the two nitrogen atoms). This backbone NH, in the hinge region between the N- and C-terminal lobes of the kinase, also donates a hydrogen-bond to the pyridine nitrogen of SB-203580, an interaction which is conserved in most other structures of inhibitors of p38α and other kinases.[3d,9] The second, longer-range hydrogen-bond is between the phenol hydroxyl and the backbone NH of Asp168, with a distance of 3.3 Å between the nitrogen and oxygen. A network of water molecules is visible in the active site, one within H-bonding distance of the aniline nitrogen (3.0 Å).

The majority of the contacts between the inhibitor and the protein are non-polar, making use of hydrophobic side chains in the N-terminal lobe of the ATP-binding site. The quinoline packs against Val38 and Ala51, while the thiazole ring makes contact with Val30. Below the plane of these rings, density is visible that has been modelled as an acetate anion from the crystallization buffer. The phenyl ring of the aniline group, and particularly its *ortho*-methyl substituent, packs in a lipophilic pocket against the methylene groups of the side chains of Ala51, Lys53 and Thr106.

Features known to favour Lck activity in this quinoline series included the thiazole, the aniline and the hydrogen-bond of the quinoline nitrogen. The coordinates of the bound conformation of compound **1** were extracted from the human p38α complex and used to build a 3D pharmacophore model (Fig. 2). Aromatic ring features and vectors were placed at the centroids of the thiazole and aniline rings. A hydrogen-bond acceptor feature was placed at the position of the quinoline nitrogen with a vector pointing towards the backbone NH of Met109. A 3-dimensional flexible pharmacophore search of the corporate database against this three-feature query was then carried out.[12] Hits were clustered to assist visual inspection. Five hundred compounds were selected and tested in the Lck enzyme assay. Although the main aim was to find new inhibitors of Lck, cross-screening was also carried out against a panel of other protein kinases, including p38α.

Compound **2** was one of the hits resulting from the search and was reproducibly active in the p38α assay with K_i of 1.6 μM.[13] Although the compound was of quite low potency, it was attractive due to its synthetic tractability and potential for optimisation. An advantage over some previous p38α inhibitor series was the lack of significant c-Jun kinase activity (Table 1). For

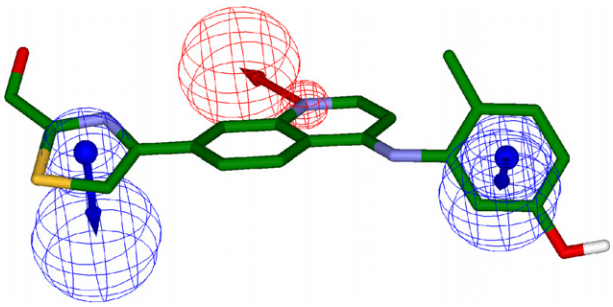

Figure 2. The pharmacophore model used in the search. Aromatic ring vectors are shown as blue arrows and H-bond acceptors as red arrows.

comparison, SB-203580 had a K_i of 18 nM against p38α and 90 nM against JNK3.

A medicinal chemistry effort began with the aim of optimising the p38α activity of the biphenyl amide (BPA) series represented by **2**. As part of this, analogues were synthesized which showed improved p38α potency (e.g., **3** and **4**, Table 1).[14]

X-ray structures of **2** and **3** were solved in complex with p38α. They adopt a novel binding mode within the ATP-site. The structure of **2** is not presented here because the electron density around the piperazine ring was insufficient to fit this part of the molecule. The rest of the inhibitor was clearly visible and the binding mode of **2** was essentially identical to that of **3**. Access to the structures at the outset of the program gave extra impetus to the medicinal chemistry effort, both to understand the SAR and to help to guide the choice of targets for synthesis.

During the pharmacophore search, the aromatic features associated with the tolyl ring and the piperazine-substituted phenyl of compound **2** were matched to the aniline and thiazole rings of compound **1**, respectively. Similarly, the H-bond donor feature of the amide carbonyl of **2** corresponded to the quinoline nitrogen of **1**. Figure 3 shows the X-ray crystal complexes of **1** and **3** overlaid using their protein backbones. These features match in the overlaid structures, confirming the pharmacophore hypothesis.

In its complex with p38α the amide of **3** adopts a trans conformation. The only hydrogen-bond between the inhibitor and the hinge region of the active site is between the amide carbonyl of **3** and the backbone amide NH of Met109 (2.7 Å between the heavy atoms). No hydrogen-bonds are made between ligand donor atoms and the carbonyls of His 107 and Met109, the 'inner' and 'outer' acceptors which are frequently seen to H-bond to inhibitors in other kinase complexes.[3d]

It has been reported that binding of certain compounds causes a flip in the p38α Gly110 backbone relative to the apo conformation.[15] This was used to explain the p38α selectivity of compounds that bind with this flip over kinases with less flexible non-glycine residues at this position. This conclusion was supported by mutagenesis data. In the complex with **3**, the density seen for Gly110 is consistent with the flipped form (Fig. 3), though no density for its Cα atom could be seen. In the flipped conformation, the Met109 carbonyl points away from the ATP site so is not available for ligand-binding. Instead, the backbone NH of Gly110 is rotated to point towards the amide carbonyl of **3**, to which it may make a second longer-range H-bond. This movement may be favoured by packing of the cyanophenyl ring against Gly110. Another feature of this complex is the density for Met109 which suggests that its side-chain adopts two distinct conformations.

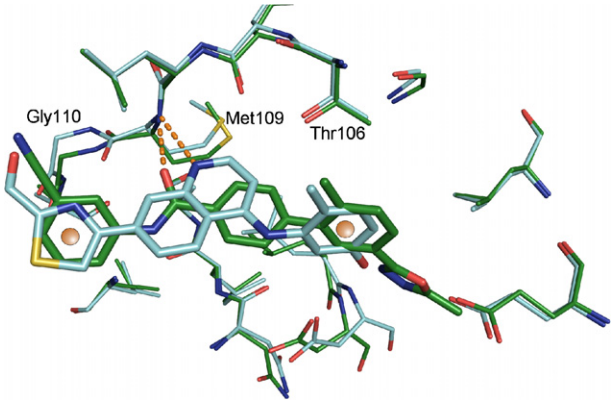

Figure 3. Overlaid complexes between p38α and compounds **1** (cyan) and **3** (green). Common pharmacophore features are indicated in orange. The backbone flip in the hinge region can be seen at Gly110.

The NH of the amide group of the inhibitor points directly away from the hinge region and towards the sugar-binding pocket, which is occupied by water molecules. The distance and angle between the NH and the nearest visible water molecule do not suggest that direct hydrogen-bonding interactions are made. The cyanophenyl ring adopts a very similar position to the thiazole of **1**, on the edge of the ATP site. Above this ring, and packing closely against it, is Val30, while below is Gly110. The *meta*-cyano group does not interact with the protein, and para substituents would extend beyond the ATP site towards solvent.

The phenyl carboxamide of **3** is planar and partly overlaps with the quinoline ring of compound **1**, making similar interactions above and below with Ala51 and Leu167. As might be expected, the rings of the *ortho*-substituted biphenyl system adopt an almost perpendicular arrangement, with an angle of ~80°.

The tolyl ring of **3** lies close to the position occupied by the aniline of **1**, albeit with a slight rotation (Fig. 3). It is especially striking that the methyl group on the tolyl of **3** overlays perfectly with the methyl group on the aniline of **1**. It fills the same small lipophilic pocket and makes the same contacts with Ala51 and Thr106.

The oxadiazole fills another cavity at the back of the ATP-site, close to Leu75 and Phe169 (Fig. 4). Its two aromatic nitrogen atoms form hydrogen-bonds to the backbone NH atoms of Asp168 and Phe169. The oxadiazole oxygen is adjacent to the acid group on the Glu71 side chain, which is presumably not a favourable electrostatic interaction, since the oxygen–oxygen distance is only 3.0 Å. The methyl substituent on the oxadiazole forms close contacts with Leu171.

The X-ray structure of **4** was also solved in p38α. Its binding mode is similar to that of **3** (Fig. 5). The amide of **4** makes the same hydrogen bond to Met109 in the hinge region as **3**, but the conformation of Gly110 in the complex with **4** is more ambiguous. The electron density suggests that it can adopt two orientations. As well as binding with the flipped Gly110 seen in the complex with **3**, **4** can also bind to the apo-like conformation (this is the conformation shown in Figure 5). The

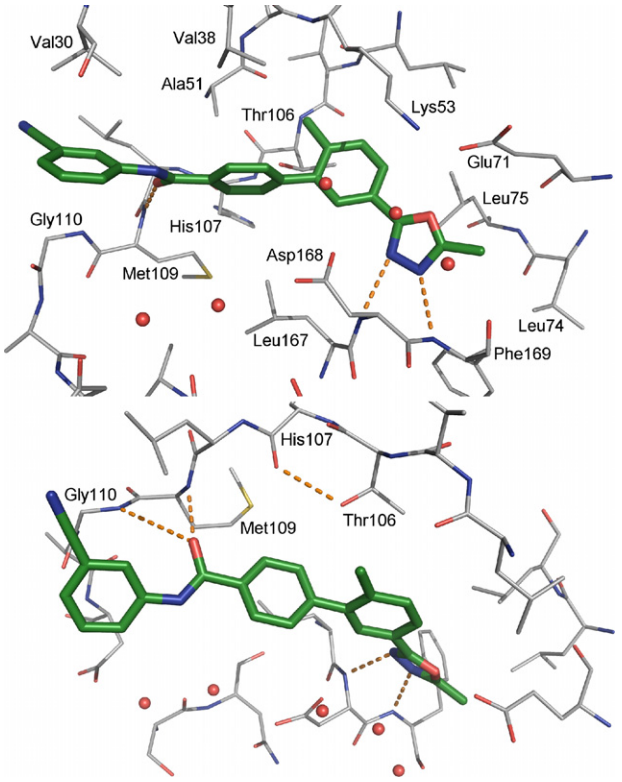

Figure 4. Two views of the X-ray structure of the complex between **3** and p38α. Orange dashes show short and possible longer-range H-bonds.

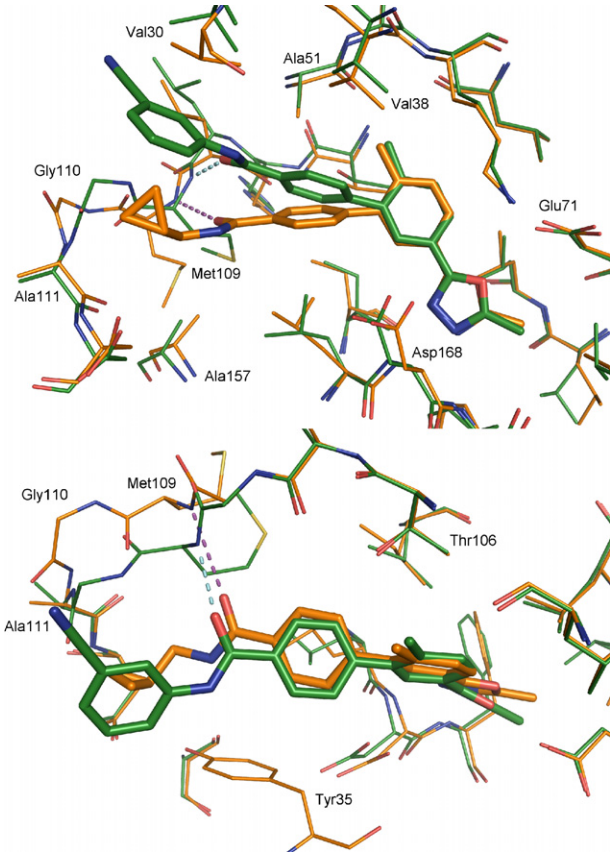

Figure 5. Structures of **3** (green) and **4** (orange) showing the rotation in the binding mode, the mobility of Gly110 and the position of Tyr35 in the complex with **4**.

difference between **3** and **4** probably arises because the cyclopropyl of **4** is small enough to pack against Ala111 in the C-terminal lobe. The larger cyanophenyl of **3** is too bulky to do this, so is forced towards Val30 in the N-terminal lobe instead, favouring the flipped Gly110. When the two structures are overlaid, the distance between the NH atoms of Met109 is 1.3 Å and the amide oxygens of the inhibitors are 2.4 Å apart. This movement is achieved by a ~12° rotation in the ligands, as well as a change in the angle between the centroids of the two phenyl rings and the oxadiazole from 121° in **3** to 116° in **4**.

Another difference between the complexes of **3** and **4** is in the conformation of the glycine-rich loop (Gly31-Ser37). In the complex with **3**, the loop adopts an extended conformation as seen in the SB-203580 complex.[9] In the complex with **4**, the loop folds across the solvent face of the ATP pocket. The sidechain of Tyr35 packs against the cyclopropyl ring of **4**, a movement of its Cα atom of approximately 8.5 Å relative to its position with **3**.

Although **3** and **4** are relatively weak inhibitors of p38α, they showed no measurable inhibition of the JNK isoforms ($K_i > 4$ μM). More potent BPAs were also inactive against the JNKs and other protein kinases.[14] The crystal structures offer several possible explanations for their selectivity for p38α.

One explanation could be related to the occupation of the back pocket by the inhibitor. It was originally thought that the small p38α gatekeeper residue, Thr106, allowed access of ligands to the back pocket. Larger residues present at that position in some other kinases would prevent binding of bulky inhibitors that access the back pocket, such as SB-203580. This view was backed by mutagenesis data in other MAP kinases, but there have since been shown to be exceptions.[16] In JNK3 it has been observed that the gatekeeper Met146 moves aside to allow binding of some inhibitors.[17] If Met146 adopted its rearranged position in JNK3 the tolyl ring of the biphenyl amides could access the back pocket. However, there would still be insufficient space for the oxadiazole because of the different backbone conformation around Leu206 in JNK3.

Another reason for the selectivity may lie in the fact that **3** and **4** are 'one-point binders' at the kinase hinge: they accept the H-bond donated by Met109, but do not donate H-bonds to either of the two possible flanking acceptor carbonyls of His107 and Gly110. This contrasts with most published kinase inhibitors, which make the donor and either the inner or outer acceptor interactions.[3d] As stated earlier, p38α may compensate for the inability of **3** to make the outer donor interaction by means of a flip of the peptide bond between Met109 and Gly110. This rotates the Gly110 carbonyl out of the binding site, removing its potential to H-bond to the inhibitor.[15] This cannot be the only factor that gives

the compounds their p38α selectivity, since **4** is still selective but can bind with and without the flip.

In addition, the Thr106 gatekeeper residue of p38α could help to offset the lack of the inner H-bond donor interaction from **3** and **4** to His107. Thr106 adopts a conformation that places the side chain hydroxyl oxygen of Thr106 3.2 Å away from the carbonyl oxygen of His107. This heteroatom-heteroatom distance is within hydrogen-bonding range. It is possible that p38α is able to bind to ligands that do not themselves make the H-bond to His107 because it makes an internal hydrogen-bond between Thr106 and His107. Kinases with gatekeeper residues other than threonine, such as the JNKs, could not compensate in this way for the lack of this interaction when binding such ligands. It is interesting to note that this Thr106 conformation is also observed in the complex with **1** and in many other published p38α structures.

It seems likely that all three factors contribute to the selectivity to some degree. One of the attractions of the biphenyl amide scaffold is its rigidity, containing as it does three aromatic rings with limited conformational freedom. This allows little opportunity for the molecule to adapt to subtly different kinase ATP sites. We believe that this is the fundamental reason for the selectivity of the biphenyl amides.

In summary, screening compounds suggested by a crystallography-based 3D pharmacophore model resulted in the discovery of a novel series of biphenyl amide inhibitors of p38α. X-ray structures of members of the biphenyl amide series provide a structural validation that the active compounds bind as the pharmacophore hypothesis intended. They also show the key features of the interactions with the active site and can be used to rationalise the selectivity of the series. The structural information gained was invaluable in guiding the optimisation of the biphenyl amides to produce compounds which proved active in in vivo models of disease. This work will be described in future publications.[14]

Acknowledgments

The authors thank Malcolm Willson and Penny A. Smee for generation of kinase enzyme data and Keith P. Ray for helpful discussions.

References and notes

1. Lee, J.; Laydon, J.; McDonnell, P.; Gallagher, T.; Kumar, S.; Green, D.; McNulty, D.; Blumenthal, M.; Heys, J.; Landvatter, S.; Strickler, J.; McLaughlin, M.; Siemens, I.; Fisher, S.; Livi, G.; White, J.; Adams, J.; Young, P. *Nature* **1994**, *372*, 739.
2. (a) Kumar, S.; Boehm, J.; Lee, J. *Nat. Rev. Drug Disc.* **2003**, *2*, 717; (b) Pargellis, C.; Regan, J. *Curr. Opin. Invest. Drugs* **2003**, *4*, 566; (c) Westra, J.; Limburg, P. *Mini-Rev. Med. Chem.* **2006**, *6*, 867.
3. (a) Hynes, J.; Leftheris, K. *Curr. Top. Med. Chem.* **2005**, *5*, 967; (b) Goldstein, D.; Gabriel, T. *Curr. Top. Med. Chem.* **2005**, *5*, 1017; (c) Peifer, C.; Wagner, G.; Laufer, S. *Curr. Top. Med. Chem.* **2006**, *6*, 113; (d) Lee, M.; Dominguez, C. *Curr. Med. Chem.* **2005**, *12*, 2979; (e) Wrobleski, S.; Doweyko, A. *Curr. Top. Med. Chem.* **2005**, *5*, 1005.
4. Golas, J.; Arndt, K.; Etienne, C.; Lucas, J.; Nardin, D.; Gibbons, J.; Frost, P.; Ye, F.; Boschelli, D.; Boschelli, F. *Cancer Res.* **2003**, *63*, 375.
5. Hennequin, L.; Thomas, A.; Johnstone, C.; Stokes, E.; Ple, P.; Lohmann, J.; Ogilvie, D.; Dukes, M.; Wedge, S.; Curwen, J.; Kendrew, J.; Lambert-van derBrempt, C. *J. Med. Chem.* **1999**, *42*, 5369.
6. Kamens, J.; Ratnofsky, S.; Hirst, G. *Curr. Opin. Invest. Drugs* **2001**, *2*, 1213.
7. Bamborough, P.; Angell, R.; Bhamra, I.; Brown, D.; Bull, J.; Christopher, J.; Cooper, A. W.; Fazal, L.; Giordano, I.; Hind, L.; Patel, V.; Ranshaw, L.; Sims, M.; Skone, P.; Smith, K.; Vickerstaff, E.; Washington, M. *Bioorg. Med. Chem. Lett.* **2007**, *17*, 4363.
8. Human p38α was expressed in *Escherichia coli* as described in Ref. 11 and purified as follows: purification was at 4 °C unless stated otherwise. Cell paste from the culture expressing hexahis-tagged p38α was lysed by sonication in Hepes, 25 mM, NaCl, 325 mM, imidazole, 25 mM, pH 7.5. The lysate was clarified by centrifugation and filtration before Ni-affinity chromatography and stepwise elution with imidazole up to 100 mM concentration. Pooled fractions were filtered before fivefold dilution into Hepes, 25 mM, DTT, 1 mM, pH 7.5 and loading onto an anion exchange Q Sepharose FF column followed by elution with a NaCl gradient to 1.0 M in the same buffer. At room temperature, the NaCl concentration of eluted fractions was made 2.0 M before application to a Phenyl Sepharose column equilibrated in Hepes, 25 mM, NaCl, 2.0 M, DTT, 1 mM, pH 7.5, and elution in a decreasing gradient of NaCl from 2 to 0 M. The eluate was diluted fivefold into Tris–HCl, 25 mM, DTT, 1 mM, pH 7.5 and loaded onto a Source Q column, equilibrated in the same buffer with 0.1 M NaCl. Elution was performed by washing successively with 0.1 and 0.2 M NaCl in the equilibration buffer and then by gradient to 0.45 M NaCl; The p38 protein was buffer exchanged into elution buffer comprising 200 mM NaCl and concentrated to 10 mg/ml. Crystallisation was at 20 °C by vapour diffusion using an equal volume of protein to well solution (100 mM ADA, pH 6.5), 180 mM $(NH_4)_2SO_4$, 18–22% PEG5000MME, 3–4% Jeffamine ED600, 2 mM β-ME) and took ~2 weeks to grow. Typically crystals were soaked in well buffer solution containing 25% PEG5000MME with 2–2.5 mM compound for ~24 h, followed by brief immersion in cryoprotectant (soaking buffer containing 10% glycerol for compound **1**, or a different cryoprotectant (100 mM ADA pH6.5, 25% PEG5000MME, 25% glycerol, 5% PEG400) for compounds **3** and **4**) prior to data collection; X-ray diffraction data were collected from each crystal at 100 K (using an Oxford Cryostream) and a Rigaku-MSC RuH2R rotating anode X-ray generator with a RAXIS IV++ image-plate detector. The data were processed with d*TREK (Pflugrath, J.W. *Acta Cryst.* **1999**, *D55*, 1718-1725) or HKL (Otwinowski, Z; Minor, W. *Methods Enzymol.*, **1997**, *276 (Macromol. Cryst. part A)*, 307–326) and structures solved using the native p38 coordinates (PDB entry 1WFC) as the initial model in refinement by REFMAC (Murshudov, G.; Vagin, A.; and Dodson, E. *Acta Cryst.* **1997**, *D53*, 240–255). The final R-factors achieved for each complex were 19.8% (compound **1**), 17.2% (compound **3**) and 16.9% (compound **4**). Coordinates have been deposited with the PDB as entries 2ZAZ, 2ZB0 and 2ZB1. Activated p38α has proved intractable to

crystallisation and no structures have yet been published, but inactive p38α readily gives crystals. These structures are frequently used to rationalise SAR of activated p38α, for example as discussed in Refs. 9 and 11.

9. PDB code 1a9u: Wang, B.; Canagarajah, J.; Boehm, J.; Kassisa, S.; Cobb, M.; Young, P.; Abdel-Meguid, S.; Adams, J.; Goldsmith, E. *Structure* **1998**, *6*, 1117.
10. PDB code 1wfc: Wilson, K.; Fitzgibbon, M.; Caron, P.; Griffith, J.; Chen, W.; McCaffrey, P.; Chambers, S.; Su, M. *J. Biol. Chem.* **1996**, *271*, 27696.
11. PDB code 1di9: Shewchuk, L.; Hassell, A.; Wisely, B.; Rocque, W.; Holmes, W.; Veal, J.; Kuyper, L. *J. Med. Chem.* **2000**, *43*, 133.
12. Pharmacophore modelling and 3D database searching was carried out using Catalyst from Accelrys Software Inc., http://www.accelrys.com.
13. p38α and JNK3 assays were carried out as described in Ref. 14. Lck activity was measured as described in Ref. 7.
14. Angell, R.; Angell, T.; Bamborough, P.; Brown, D.; Brown, M.; Buckton, J.; Cockerill, S.; Edwards, C.; Jones, K.; Longstaff, T.; Smee, P.; Smith, K.; Somers, D.; Walker, A.; Willson, M. *Bioorg. Med. Chem. Lett.* **2008**, *18*, 324.
15. Fitzgerald, C.; Patel, S.; Becker, J.; Cameron, P.; Zaller, D.; Pikounis, V.; O'Keefe, S.; Scapin, G. *Nat. Struct. Biol.* **2003**, *10*, 764.
16. (a) Eyers, P.; Craxton, M.; Morrice, N.; Cohen, P.; Goedert, M. *Chem. Biol.* **1998**, *5*, 321; (b) Lisnock, J.; Tebben, A.; Frantz, B.; O'Neill, E.; Croft, G.; O'Keefe, S.; Li, B.; Hacker, C.; deLaszlo, S.; Smith, A.; Libby, B.; Liverton, N.; Hermes, J.; LoGrasso, P. *Biochemistry* **1998**, *37*, 16573.
17. Scapin, G.; Patel, S.; Lisnock, J.; Becker, J.; Lograsso, P. *Chem. Biol.* **2003**, *10*, 705.